Missense variants of *FBN2* associated with congenital arachnodactyly in three Chinese families

Yu Sui, Yongping Lu, Meina Lin, Xinren Chen, Xiang Ni, Huan Li, Miao Jiang [*]

Department of Medical Genetics, Liaoning Institute of birth health and development, Reproductive Hospital of China Medical University, 10 Puhe street, Huanggu District, Shenyang city, Liaoning Province 110031, China

ARTICLE INFO

ABSTRACT

Background: Congenital contractural arachnodactyly (CCA) is a rare autosomal dominant disorder caused by pathogenic variants of Fibrillin-2 (*FBN2*) gene. This study aimed to investigate the variants in three Chinese families with CCA.

Methods: Next-generation sequencing analysis and Sanger sequencing of exons 24–35 of *FBN2* (NM_001999.4) were performed on the three CCA pedigrees. The pathogenicity of the variants was assessed using ACMG criteria and predicted using an in-silico program.

Results: A novel heterozygous substitution (NM_001999.4: c.3230G > A; NP_001990.2 p. Cys1077Tyr) was identified in all patients from pedigree A, but not in healthy family members. The variant was found to be pathogenic. Additionally, in pedigree B (NM_001999.4: c.4222G > A; NP_001990.2: p.Asp1408Asn) and C (NM_001999.4: c.3170G > A; NP_001990.2: p.Gly1057Asp), and the previously reported variants were detected. Variants affecting cysteine residues may disrupt disulfide bridging, leading to a weakened microfibril scaffold, resulting in CCA phenotypes. High phenotypic heterogeneity was observed among different families, and there was little correlation between the genotype and phenotype.

Conclusion: This study describes three large families with CCA caused by missense variants in the *FBN2* gene. Phenotypic variations were observed among different pedigree groups, and further research is needed to investigate the underlying reasons for these variations.

1. Introduction

Congenital contractural arachnodactyly (CCA, OMIM: 121050) is a rare, autosomal dominant disorder [1] that has been genetically linked to Fibrillin-2 (*FBN2*) gene [2–4]. *FBN2* is located at 5q23–31 and encodes Fibrillin-2 which is one of the components of microfibrils in the extracellular matrix [5] that provides strength and flexibility to the connective tissues that form the body's joints and organs [6]. Mutations in *FBN2* can reduce the production or alter the function of fibrillin-2 protein, thereby directly affecting the function of microfibrils and leading to CCA phenotypes [7].

CCA exhibits a wide range of clinical manifestations, including a Marfan syndrome appearance characterized by a tall, slender, and asthenic appearance, as well as skeletal abnormalities such as arachnodactyly, dolichostenomelia, pectus deformities, and kyphoscoliosis [6]. Most patients with CCA display mild flexion contractures of the elbows, knees, and hips, as well as mild muscular hypoplasia, particularly in the calf muscles [8]; kyphosis/scoliosis is observed in approximately half of all affected individuals [9]. Another distinctive feature of CCA is "crumpled" ears. According to a previous clinical scoring system for CCA, only crumpled ears, arachnodactyly and camptodactyly showed statistical significance when scoring the typical phenotypes of CCA [10]. However, this phenotype varied widely even among the family members carrying the same pathogenic variant: from "crumpled" to normal ears [11]. Similarly, Callewaert et al. reported varied arachnodactyly of the fingers in patients within the same family who showed no signs of arachnodactyly (Pedigree E: Patients II2 vs. III2 and III-1) [12].

CCA patients exhibit significant inter- and intrafamilial phenotype heterogeneities, but little is known about the relationships between

genotype and phenotypes. In this report, we have described pathogenic variants identified in three Chinese CCA families and explore the possible reasons for the observed phenotype heterogeneity.

2. Materials and methods

For each family, the probands, who were suspected of having CCA were referred to our research team and underwent evaluation by specialists and a medical geneticist (Miao Jiang), leading to a confirmed diagnosis of CCA. Complete family histories were obtained and all of the participating members underwent phenotypic examination for CCA.

2.1. DNA extraction

Informed consent was obtained and blood samples were collected from family members. We also recruited 100 healthy individuals from the same geographical area as the patients to determine whether the new mutations causing amino acid changes were innocuous polymorphisms or pathogenic mutations. Genomic DNA was extracted from the blood samples using a DNA Isolation Kit for Mammalian Blood (Tiangen Biotech, China).

2.2. Next generation sequencing analysis

NGS analysis was performed by Chigene Translational Medical Research Center Co. Ltd. (Beijing, China). The NGS analyses included three probands and three controls. After obtaining the NGS results, we conducted data cleansing and collation using the dplyr() package of the R software. First, we removed variations present in both the patients and normal controls within each family. Next, we included sequencing results of variants with medium quality, defined as: 1) depths of sequencing between 20 reads to 400 reads, and 2) the variant allele reads were between 30 and 70 % of the total reads. We further included the remaining variants based on the following criteria: 1) frequencies less than 0.001 in the Thousand Human Genome frequency (China) (https://www.ncbi.nlm.nih.gov/variation/tools/1000genomes/) and ExAC(Exome Aggregation Consortium) database(http://exac.broadinstitute.org/); 2) exclusion criteria: variants predicted by in-silico programs to be protein alterations that are either tolerated or potentially harmless, synonymous variants, variants with a minor allele frequency greater than or equal to 5 %, indicating a possible polymorphic variation [13], variants located in non-coding areas including introns and intergenic regions.

After filtering the potentially pathogenic variants based on the quality of the NGS results, we searched the SNP database (https://www.ncbi.nlm.nih.gov/snp)to exclude any reported polymorphisms. For the remaining genes with possible pathogenic alleles identified from the NGS sequencing data, we examined their functions using the OMIM (https://www. ncbi. nlm. Nih. gov/omim/) and GeneCards (https://www.genecards.org/) databases to assess their potential contributions to the phenotypic heterogeneity observed in the family.

2.3. PCR amplification and sanger sequencing of possible pathogenic alleles of FBN2

In order to validate the presence of any identified variants, we performed PCR amplification of DNA samples from the family members. The PCR amplification systems used are provided in the Supplementary Materials (Table S1). Additionally, to rule out the possibility that the identified variant was a polymorphism, we performed Sanger sequencing of DNA samples from 100 healthy controls (Sangon Biotech, Shanghai, China). The sequencing results were compared with those of the wild-type sequence submitted to GenBank (accession number NM_001999.4). Once a pathogenic mutation was identified, genetic counseling was offered to family members. All of the participants in the study provided signed informed consent for both genetic testing and for

making their clinical and genetic data available for research purposes. The study protocol and consent forms were approved by the local research ethics committee, particularly the Ethics Committee of the Key Laboratory of Reproductive Health in Liaoning Province.

2.4. Variants analyses

We evaluated the pathogenicity of the variants based on the ACMG criteria and in silico programs(PROVEN, PolyPhen, MutationTaster and MutationAssessor, FATHMM, and M-CAP) [14–17]. Additionally, a search for human *FBN2* homologs was conducted using BLAST on NCBI web site (http://www.ncbi.nlm.nih.gov). The identified proteins were aligned, and a phylogenetic tree was reconstructed with MEGA11.0 using the neighbor-joining method in pedigree A [18,19].

2.5. Molecular modeling of FBN2 protein

The amino acid sequence of FBN2 was obtained from the UniProtKB database (http://www.uniprot.org/uniprot/P35556) and the domain structure was determined using Simple Modular Research. Tool (SMART) [20]. Search for structural repeats and multiple sequence alignment of calcium-binding epidermal growth factor (Ca_EGF) motifs 11–22 was performed using Rapid Automatic Detection and Alignment of Repeats (RADAR; http://www.ebi.ac.uk/Tools/pfa/radar/). The three-dimensional structure of FBN2 was modeled using SWISSMODEL [21], with the protein structure of a Ca_ EGF-like domain pair from the neonatal region of human FBN1 serving as a template (PDB: 2w86). The identity between human FBN1 and FBN2 sequences was 67.259 %. The structures of wild-type and mutant FBN2 were visualized using PyMOL (PyMOL Molecular Graphics System v. 1.8.x).

3. Results

### 3.1. Phenotypes and pathogenic variant of Pedigree A

Pedigree A consisted of four generations and 5 CCA patients (Fig. 1-1). No patient in pedigree A had a "Marfan syndrome " appearance, such as being tall, slender, or asthenic. All the patients in this family had a normal height (approximately 1.60–1.65 m for females, and 1.70–1.75 m for males) (Table 1). Upon examination of the dorsal/palmar side of the palm, the proband's two hands presented with mildly clubbed fingers (PP4). Only the little fingers of the proband's two hands showed significant arachnodactyly phenotype. Among the other four fingers, the thumb did not show a significant flexed phenotype, whereas the middle three fingers showed mild contracture at the first finger joint, which prevented the fingers from lying flat on the desktop (Fig. 3). The palm showed mild finger muscle dysplasia, which resulted in arachnodactyly. There were no signs of joint contractures in the elbows, hips, or knees, crumpled ears or curly hair, pectus deformities, or kyphoscoliosis (Fig. 3). (Table 1). Unaffected members of Pedigree A showed no CCA phenotype, and no overt body-weight phenotype was found among unaffected members of Pedigree A (Table 1).

Whole-exome sequencing revealed a novel G → A variant at nucleotide position c.3230 in exon 25 in pedigree A, resulting in a cysteine-to-tyrosine substitution at amino acid residue 1077 (NM_001999.4: c.3230G > A; NP_001990.2p. Cys1077Arg) (Fig. 2–1). This novel variant was evaluated as "Likely pathogenic" according to the ACMG criteria (1 moderate PMs: PM2; 4 supporting PPs:PP1 ∼ 4): This variant was not reported in global-scale initiatives for variant annotation, such as the Exome Aggregation Consortium (ExAC) or the 1000 Genomes Project (PM2); Mutation analysis confirmed the segregation of this variants with CCA, and it was shared by multiple cases in pedigree A (PP1); By performing a BLAST search, ten proteins in the FBN2 subfamily were identified. To understand the evolutionary conservation of *FBN2* gene among mammals, we generated phylogenetic trees, and found that this gene is highly conserved in mammals. (Fig. S1). The p.

Table 1

Phenotypes Heterogeneities of family members.

Genotype	Patho	MAF-like	Height (m)	Contr-1	Contr-2	JD	Exter	muscle hypopl	ARD/MVP	Ky/Sco	Pectus def	Club	Ara	Camp	Reference
c.3230G p.C1077	Wild type	-	F: 1.60–1.67 M:1.70–1.78	-	-	-	-	-	-	-	-	-	-		UMP in Pedigree A
c.3230G > A p. C1077Y	variant	-	F: 1.60–1.65 M:1.70–1.75	+	-	-	-	-	-	-	-	-	+	+	Patients in Pedigree A
c.3229 T > G p. C1077G	Variant	-	F: 1.60–1.70 M:1.70–1.85	+++	-	-	-	-	-	-	-	+	+	+	[1]Guo
c.4222G p. D1408	Wild type	-	F: 1.65–1.75 M:1.80–1.85	-	-	-	-	-	-	-	-	-	-	-	UMP in Pedigree B
c.4222G > A p. D1408N	Variant	-	NA	+	+	-	+	-	-	+	-	-	+	+	[2] Callewaert
		+	M:1.90—1.95	+	-	-	-	-	-	-	-	-	+	+	Patients in Pedigree B
c.3170G p. G1057	Wild type	-	F: 1.60–1.65 M:1.75–1.82	-	-	-	-	-	-	-	-	-	-	-	UMP in Pedigree C
c.3170G > A p. G1057D	Variant	++	NA	+++	+	++	+/−	+	-	-	-	-	+	+	[3] Park
		++	M:1.80–1.95 F:1.65–1.70	+++	-	-	+	+	-	+	+	+	+	+	Patients in Pedigree C

Contr-1: Contractual of fingers and toes; Contr-2: Contractual of the elbows, hips and knees; JD: Joint dislocation; muscle hypopl: muscular hypoplasia; ARD: aortic root dilatation; MVP:mitral valve prolapse; Pectus def, pectus deformity; Ky/Sco: Kyphoscoliosis/Scoliosis; MAF-like: MarFan syndrome like phenotype; Ara:arachnodactyly Club: Clubbed fingers and toes; Camp: Camptodactyly.

1-1: Pedigree A

1-2: Pedigree B
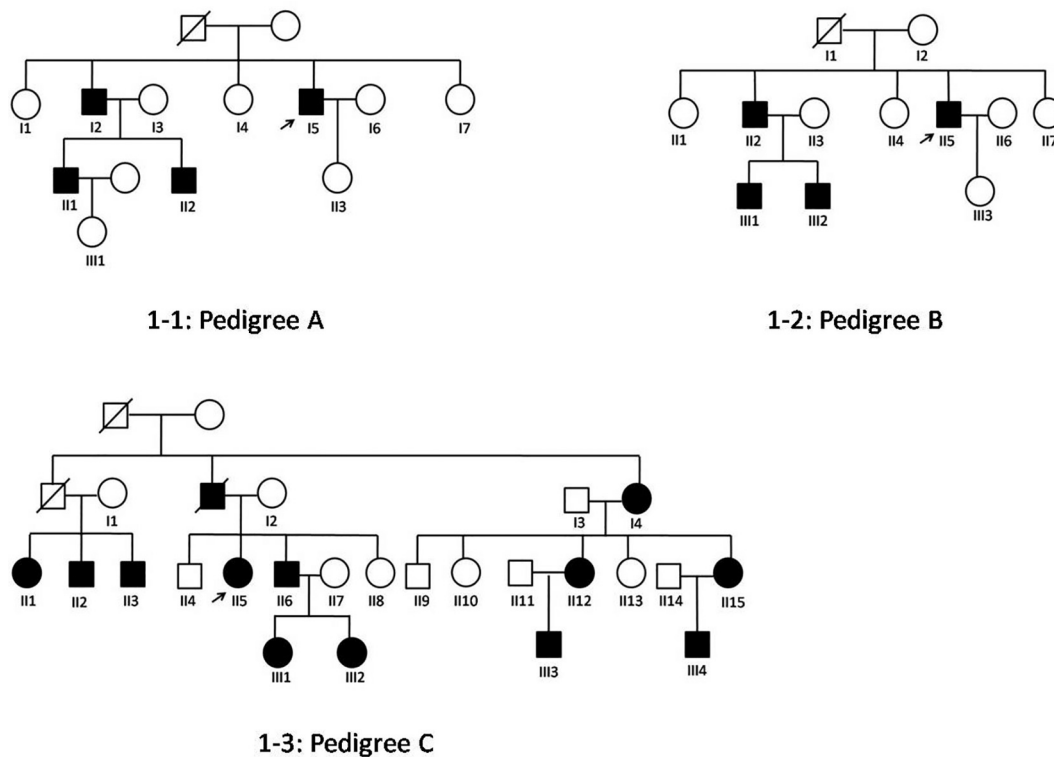
1-3: Pedigree C

Fig. 1. Pedigree of 3 CCA families.
Fig. 1-1 Pedigree A.
Fig. 1-2 Pedigree B.
Fig. 1-3 Pedigree C.
Black symbol represents affected individuals, and an arrow indicates the proband.

Cys1077Tyr (NM_001999. NC_000005.10: c.3230G > A) variant occurred in exon 25 of *FBN2*. Alignment of numerous species revealed that this region is highly conserved (Fig. S2). In silico prediction programs indicated that this variant is pathogenic. (Table S2) (PP3).

3.2. Phenotypes and pathogenic variant of Pedigree B

The patients in pedigree B did not exhibit typical features of Marfan syndrome or CCA. In particular they did not have a slender, asthenic appearance. However, the male patients (but not female patients) had a higher median body height (>1.9 m) with a robust body structure. Unaffected individuals were found to be taller than the general population (Female: 1.65–1.75; Male:1.72–1.83), and did not present any CCA phenotypes (Table 1). The proband presented with the typical arachnodactyly phenotype, characterized by disproportionately slender and long fingers and toes; congenital contractures were only observed in the fingers (Fig. 4–1,2,3,4). The long and slender fingers showed a slight degree of flexion contracture at the second knuckle. Only the little fingers of the patient's hands exhibited a typical contractual phenotype. Pedigree B consisted of four generations and 4 CCA patients (Fig. 1-2). A G-to-A substitution at nucleotide position c.4222 resulted in the substitution of aspartic acid for asparagine at position 1408 (NM_001999.4: c.4222G > A; NP_001990.2: p. Asp1408Asn) (HGMD:CM091472) (Fig. 2–2). This variant was detected in all patients but not in healthy controls. According to the ACMG criteria, this variant was classified as "pathogenic" (1strong PS: PS1). The pedigree B variant was also previously reported by Callewaert et al. in 2009 and was demonstrated to be "pathogenic" based on the clinical phenotype and molecular genetic analyses (PS1).

3.3. Phenotypes and pathogenic variant of Pedigree C

Pedigree C included 4 generations and 12 CCA patients (Fig. 1-3). In pedigree C, a G-to-A substitution at nucleotide position c.3170 resulted in the substitution of glycine for aspartic acid at position 1057 (NM_001999.4: c.3170G > A; NP_001990.2: p. Gly1057Asn) (HGMD CM980734) (Fig. 2–3). According to the ACMG criteria, this variant was classified as "pathogenic" (1strong PS: PS1). This was previously reported by Park et al. [22]. The patients in pedigree C exhibited a tall and slender build, slender and contractual clubbed fingers and toes (Fig. 5:1–3), and crumpled ears (Fig. 5–4). Scoliosis and associated spinal depression were also observed (Fig. 5–5). Some patients in this pedigree had aortic root dilatation (II3 and II1). Unaffected members of pedigree C did not present any CCA phenotype, no overt body-weight phenotype was found (Table 1).
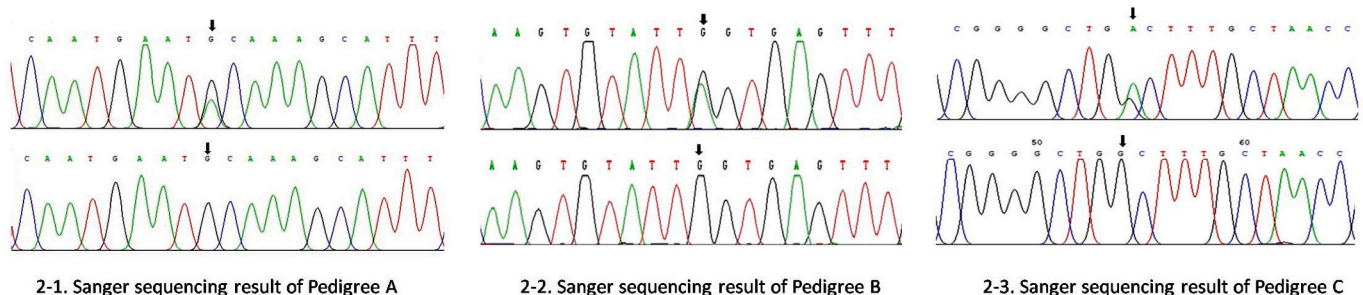
4. Discussion

CCA may exhibit skeletons similar to those of Marfan syndrome [23,24]. These syndromes are caused by mutations in two different genes belonging to the fibrillin family: fibrillin-1 and 2 (*FBN1* and *FBN2)* [25]. *FBN1* encodes fibrillin-1, which is an important component of connective tissue [26]. *FBN2* encodes fibrillin-2 protein, which is

Fig. 3. Phenotypes of proband in pedigree A.
Fig. 3–1 Full length portrait of the proband in pedigree A.
Fig. 3–2 Left side profile of the proband in pedigree A.
Fig. 3–3 Right side profile of the proband in pedigree A.
Fig. 3–4 Dorsum manus of the proband in pedigree A.
Fig. 3–5 Palm of the proband in pedigree A.

present in the core of adult microfibril bundles [27–29]. Fibrillins contribute to the elasticity and strength of connective tissue that supports the body's organs and joints [30].

Human FBN2 protein consists of 2912 amino acids and contains 3 epidermal growth factor-like (EGF) domains, 43 calcium-binding consensus sequences (cb_EGF domains) and seven transforming growth factor β1 binding protein-like (TB) domains. The cb_EGF domain contains six highly conserved cysteine residues that form disulfide bridges, ensuring the stability and folding of the domains [31–33]. These cysteine-rich glycoproteins are the main structural components of microfibrils, which act as scaffolds for elastin deposition and modification during the formation of elastic fibers [34]. Most pathogenic variants are associated with the CCA cluster between exons 23 and 34 (cb_EGF10–cb_EGF20) of *FBN2* [35]. Approximately 45 % of *FBN2* pathogenic mutations are missense mutations that result in the replacement of cysteine residues with other amino acids. These variants disrupt the normal disulfide bridging within and between domains, leading to increased susceptibility to proteolysis and exposure to cryptic

2-1. Sanger sequencing result of Pedigree A

2-2. Sanger sequencing result of Pedigree B

2-3. Sanger sequencing result of Pedigree C

Fig. 2. Sanger sequencing results of 3 CCA pedigrees.
Fig. 2–1 Sanger sequencing result showing a heterozygous change c.3230G > A in *FBN2*.
Fig. 2–2 Sanger sequencing result showing a heterozygous change c.4222G > A in FBN2.
Fig. 2–3 Sanger sequencing result showing a heterozygous changec.3170G > A in FBN2.
Sanger sequence analyses of affected individuals and normal unaffected controls. The mutant and wild-type variants are indicated by black arrows.

Fig. 4. Phenotypes of proband in pedigree B.
Fig. 4–1 Frontal image of the patient of proband in pedigree B.
Fig. 4–2 Dorsum manus of the proband in pedigree B.
Fig. 4–3 Palm of the proband in pedigree B.
Fig. 4–4 Foot of the proband in pedigree B.

Fig. 5. Phenotypes of proband in pedigree C.
Fig. 5–1,2 Slender, contractual clubbed fingers.
Fig. 5–3 Slender, contractual clubbed toes.
Fig. 5–4 Crumpled ears presented among all patients.
Fig. 5–5 Scoliosis and the resultant depressed of the spine.

cleavage sites. This weakens the microfibril scaffold and reduces the structural integrity of fibrillin-2, ultimately causing the defects associated with contractural arachnodactyly [36–41]. In our study, we identified a novel missense variant (c.3230G > A p. Cys1077Tyr) in pedigree A, which was classified as a "likely pathogenic" mutation based on the ACMG criteria (Fig. 2–1). Guo et al. [6] reported a pathogenic variant at the same amino acid position (p. Cys1077Gly).

There are high phenotype heterogeneities but few genotype-phenotype relationships between CCA pedigrees. Unlike typical CCA phenotypes, patients in pedigree A exhibited milder arachnodactyly and camptodactyly accompanied by hypoplastic muscles in the fingers (Fig. 3, Table 1: Pedigree A), no contractures of the elbows, hips, and knees, and no crumpled ears or kyphoscoliosis (Fig. 3, Table 1: Pedigree A). In a previous study reported by Guo et al. [6], the pedigree phenotypes were limited to joint contractures of the fingers but were more severe (Table 1:Reference 1, Fig. 6: c. 3229 T > C, p.Cys1077Gly), which included arachnodactyly of the fingers and toes. Severe contraction of the connective tissue of the fingers led to the inability of the second phalanx to extend, resulting in some patients having a semi-clenched palm shape. Muscular hypoplasia of the fingers led to clubbed fingers in some patients. Examination of the palmar side revealed that these patients presented with severe arachnodactyly phenotypes. No neurological or cardiovascular abnormalities, external ear malformations, or eye abnormalities (Table 1: Reference 1) were found in our study. Although the novel pathogenic variant in pedigree A affects the same amino acid residue as one of the previously reported mutations [6], the extent and severity of the symptoms of these two families were not consistent. Patients in pedigree A had milder symptoms, whereas Guo et al. reported patients with typical and more severe contractural fingers [6] (Fig. 3, Table 1: Pedigree A and Reference 1). Other phenotypes such as pectus deformity, dolichostenomelia, cardiovascular and ocular malformations, and muscle hypoplasia varied among individuals and cannot be used as reliable diagnostic clues for CCA.

High phenotypic heterogeneities have also been observed among different CCA families. Patients with pedigree B exhibited atypical CCA phenotypes. Instead of having thin and slim statures, all patients were extremely tall (over 1.9 m) with stalwart statures and rough features and mild arachnodactyly phenotypes, characterized by disproportionately slender and elongated fingers and toes. Congenital contractures were observed only in the clubbed fingers (Fig. 4, Table 1: Pedigree B). Conversely, patients reported by Callewaert et al. shared the same pathogenic variant c.4222G > A p. Asp1408Asn (Fig. 2–3), which potentially affects the 23th cbEGF-like/vWA matrilllin domain, disrupting the consensus sequence DLDE, impairing phosphatase activity, and ultimately leading to CCA phenotypes [11,42], and exhibited typical CCA phenotypes, including arachnodactyly, camptodactyly, pronounced joint contracture, scoliosis, generalized muscle hypoplasia, and additional unique features like cleft palate and highly arched palate [11](Table 1:Reference 2). In contrast, patients from pedigree C in our research and patients reported by Park et al. [22] shared the same variation(c.3170G > A p. Gly1057Asp)(Fig. 2: NM_001999.4: c.4222G > A; NP_001990.2: p.Asp1408Asn) and exhibited minimal phenotypic differences; both pedigree groups featured slender and tall stature, severe contractures in the fingers and toes, and some patients showed crumpled ears (Fig. 5, Table 1: Pedigree C and Reference 3). Interestingly, this unique variant does not occur in functionally related cbEGF-like or Pfam: TB domains but still results in severe clinical phenotypes. Park et al. [22] reported two patients with CCA with the same pathogenic mutations but exhibiting opposite ear phenotypes (Patient 279 vs. Patient 103). Interestingly, patient 279 suffered from bilateral progressive hearing loss, and his daughter had crumpled helical ears (patient 276) and a severe form of crumpled ears to normal ears (e.g., patients in pedigree M: III-1 vs. II-2). Patients described by Park et al. also presented with unique phenotypes, such as pes planovaglus, bilaterally frequent dislocations of the elbows, and dislocated patellae [22]. Some patients also suffered arthritis [22]. Furthermore, according to previous
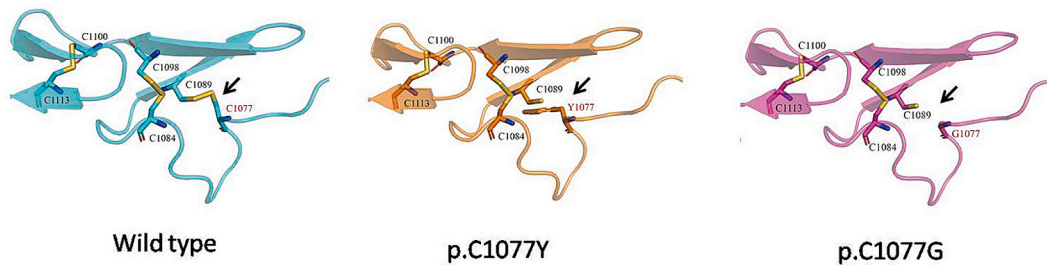
Fig. 6. The intact and broken disulfide bond in wild type and variant type.
Fig. 6 The intact and broken disulfide bonds are indicated by black arrows.

research, contractures of the large joints (elbows, hips, and knees) may be another characteristic phenotype, with the accumulation of clinical cases and continued investigation in the future [10]. However, this phenotype differs even in patients with the same pathogenic variant. For example, Callewaert et al. [11] reported a patient with CCA with a large joint contracture; however, this phenotype was absent in our research on pedigree B (Fig. 4, Table 1: Pedigree B and Reference 2). Similarly, Park et al. [22] reported a CCA patient with dislocations of the elbows and patellae; however, the patients in our study on pedigree C did not exhibit a similar phenotype (Fig. 5, Table 1: Pedigree C and Reference 3). Thus, it is generally accepted that arachnodactyly and camptodactyly of the fingers and toes are characteristic phenotypes of CCA. However, the onset and severity of symptoms can vary significantly even among individuals within the same family with the same mutation. Patients with CCA display significant phenotypic variability, both between families and within the same family, and there is minimal correlation between the genotype and phenotype. Moreover, there are currently no FBN2 knockout animal models that can fully replicate the clinical characteristics of CCA in humans [43]. Homozygous knockout mouse models only show syndactyly and transitory neonatal contractures without external ear deformities, arachnodactyly, or spinal anomalies. Conversely, *FBN2* hemizygous mice failed to exhibit abnormal phenotype [44]. The diagnosis of CCA should involve a combination of phenotypic evaluation and molecular biology techniques.

The homology between *FBN2* to *FBN1* suggests that diseases caused by variants in these two genes may share similar pathogenic mechanisms [45,46]. In the case of Marfan syndrome, some cases are believed to occur through a dominant-negative mechanism that can influence the phenotypes and expressivity of patients [39,44,47–50]. The mutant allele product interferes with the function of the wild-type allele, disrupting the function of both normal and mutant alleles [45,46,48,51]. Similarly, studies assessing *FBN2* allele expression levels in CCA cell strains have shown that mutant expression is greater than non-mutant allele expression [48]. This suggests that reduced expression of one normal *FBN2* allele could contribute to CCA pathogenesis and lead to phenotypic heterogeneity [44]. In other words, an individual in a family with CCA may be more severely affected if normal fibrillin-2 production is diminished, whereas individuals in our CCA families (pedigrees A and B) may have a lower amount of mutant fibrillin-2 production, resulting in milder phenotypes [48]. It would be valuable to test the ratio of mutant/normal allele expression of *FBN2* in future research, as individuals with the same variants could serve as good models for identifying modifiers of CCA genotypes. Additionally, it is important to consider that genetic variants may not be the sole factors influencing clinical manifestations. Environmental, genetic, and epigenetic factors, such as methylation and their interactions, should also be considered [52,53].

4.1. Conclusion

This study highlighted three Chinese families with CCA with significant phenotypic variations. Patients in the two families exhibited milder CCA phenotypes than those in previous reports. Further investigations are needed to explore the relationship between the expression ratio of the mutant/normal allele of *FBN2* and the differences in clinical phenotypes.

Ethics approval statement

The research was performed with the approval of the Ethics Committee of Reproductive Health of Liaoning Province and China Medical University, and participants gave written consent to participate after being informed of the nature of the research. All methods were carried out in accordance with the Declaration of Helsinki.

Patient consent statement

Signed informed consent was obtained from all members of the studied family for publication of personal and clinical information (images included) in this research.

Permission to reproduce material from other sources

All authors confirmed the Permission of reproduce material from other sources.
All authors confirm the following:
The manuscript has not been previously submitted.
The research meets ethical guidelines.
The paper is submitted solely to this journal.
Ethics approval and consent to participate:
Consent for publication:

Author's contributions

MJ designed the project, collected the clinical data, organized the experimental results and evaluated the phenotypes for this family. YS wrote the paper, collected the clinical data, organized the experimental results, conducted the PCR experiments and sequencing analysis, interpreted the data, and evaluated the phenotypes for the family with CCA. YPL organized the experimental results and interpreted the data. MNL organized the experimental results and interpreted the data. XN conducted the PCR experiments and sequencing analysis. XR Chen interpreted the data. HL conducted the PCR experiments and sequencing

analysis. All authors read and approved the final manuscript.

CRediT authorship contribution statement

Yu Sui: Writing – review & editing, Writing – original draft, Visualization, Validation, Supervision, Methodology, Investigation, Funding acquisition, Formal analysis, Data curation, Conceptualization. **Yongping Lu:** Supervision, Software, Methodology, Investigation, Funding acquisition, Formal analysis, Data curation, Conceptualization. **Meina Lin:** Project administration, Methodology, Investigation, Funding acquisition, Formal analysis, Conceptualization. **Xinren Chen:** Software, Project administration, Methodology, Investigation, Data curation. **Xiang Ni:** Validation, Project administration, Methodology, Investigation, Formal analysis. **Huan Li:** Methodology, Investigation, Formal analysis, Data curation. **Miao Jiang:** Writing – review & editing, Writing – original draft, Visualization, Validation, Supervision, Software, Resources, Project administration, Methodology, Investigation, Funding acquisition, Formal analysis, Data curation, Conceptualization.

Declaration of competing interest

The authors declare that there is no competing interest in this research.

Data availability

Data will be made available on request.

Appendix A. Supplementary data

Supplementary data to this article can be found online at https://doi.org/10.1016/j.ymgmr.2024.101140.

References

[1] P.A. Gupta, et al., Ten novel FBN2 mutations in congenital contractural arachnodactyly: delineation of the molecular pathogenesis and clinical phenotype, Hum. Mutat. 19 (1) (2002) 39–48.

[2] B. Lee, et al., Linkage of Marfan syndrome and a phenotypically related disorder to two different fibrillin genes, Nature 352 (6333) (1991) 330–334.

[3] H.C. Dietz, et al., Marfan syndrome caused by a recurrent de novo missense mutation in the fibrillin gene, Nature 352 (6333) (1991) 337–339.

[4] P. Tsipouras, et al., Genetic linkage of the Marfan syndrome, ectopia lentis, and congenital contractural arachnodactyly to the fibrillin genes on chromosomes 15 and 5. The international Marfan syndrome collaborative study, N. Engl. J. Med. 326 (14) (1992) 905–909.

[5] E.A. Putnam, et al., Fibrillin-2 (FBN2) mutations result in the Marfan-like disorder, congenital contractural arachnodactyly, Nat. Genet. 11 (4) (1995) 456–458.

[6] X. Guo, et al., Whole exome sequencing identifies a novel missense FBN2 mutation co-segregating in a four-generation Chinese family with congenital contractural arachnodactyly, BMC Med. Genet. 17 (1) (2016) 91.

[7] J.M. Hurle, et al., Elastin exhibits a distinctive temporal and spatial pattern of distribution in the developing chick limb in association with the establishment of the cartilaginous skeleton, J. Cell Sci. 107 (9) (1994) 2623–2634.

[8] E. Tun Bilek, Y. Alanay, Congenital contractural arachnodactyly (Beals syndrome), Orphanet J. Rare Dis. 1 (2006) 20.

[9] M.Y. Frédéric, et al., The FBN2 gene: new mutations, locus-specific database (universal mutation database FBN2), and genotype-phenotype correlations, Hum. Mutat. 30 (2) (2009) 181–190.

[10] I. Meerschaut, et al., A clinical scoring system for congenital contractural arachnodactyly, Genet. Med. 22 (1) (2020) 124–131.

[11] B.L. Callewaert, et al., Comprehensive clinical and molecular assessment of 32 probands with congenital contractural arachnodactyly: report of 14 novel mutations and review of the literature, Hum. Mutat. 30 (3) (2009) 334–341.

[12] B. Callewaert, Congenital Contractural Arachnodactyly, University of Washington, Seattle, Seattle (WA), 2001 Jan 23, pp. 1993–2024.

[13] M. Imelfort, et al., Discovering genetic polymorphisms in next-generation sequencing data, Plant Biotechnol. J. 7 (4) (2009) 312–317.

[14] P.C. Ng, S. Henikoff, Predicting deleterious amino acid substitutions, Genome Res. 11 (5) (2001) 863–874.

[15] P.C. Ng, S. Henikoff, SIFT: predicting amino acid changes that affect protein function, Nucleic Acids Res. 31 (13) (2003) 3812–3814.

[16] I.A. Adzhubei, et al., A method and server for predicting damaging missense mutations, Nat. Methods 7 (4) (2010) 248–249.

[17] J.M. Schwarz, et al., MutationTaster evaluates disease-causing potential of sequence alterations, Nat. Methods 7 (8) (2010) 575–576.

[18] J.D. Thompson, D.G. Higgins, T.J. Gibson, CLUSTAL W: improving the sensitivity of progressive multiple sequence alignment through sequence weighting, position-specific gap penalties and weight matrix choice, Nucleic Acids Res. 22 (22) (1994) 4673–4680.

[19] K. Tamura, et al., MEGA4: molecular evolutionary genetics analysis (MEGA) software version 4.0, Mol. Biol. Evol. 24 (8) (2007) 1596–1599.

[20] C.P. Ponting, et al., SMART: identification and annotation of domains from signalling and extracellular protein sequences, Nucleic Acids Res. 27 (1) (1999) 229–232.

[21] F. Kiefer, et al., The SWISS-MODEL repository and associated resources, Nucleic Acids Res. 37 (Database issue) (2009) D387–D392.

[22] E.S. Park, et al., Clustering of FBN2 mutations in patients with congenital contractural arachnodactyly indicates an important role of the domains encoded by exons 24 through 34 during human development, Am. J. Med. Genet. 78 (4) (1998) 350–355.

[23] A. Jurko Jr., et al., Congenital contractural arachnodactyly (Beals-Hecht syndrome): a rare connective tissue disorder, Wien. Klin. Wochenschr. 125 (9–10) (2013) 288–290.

[24] M. Inbar-Feigenberg, et al., Beals syndrome (congenital contractural arachnodactyly): prenatal ultrasound findings and molecular analysis, Ultrasound Obstet. Gynecol. 44 (4) (2014) 486–490.

[25] M.Y. Frédéric, et al., The FBN2 gene: new mutations, locus-specific database (universal mutation database FBN2), and genotype-phenotype correlations, Hum. Mutat. 30 (2) (2009) 181–190.

[26] J.J. Doyle, et al., A deleterious gene-by-environment interaction imposed by calcium channel blockers in Marfan syndrome, Elife (2015) 4.

[27] H. Zhang, et al., Structure and expression of fibrillin-2, a novel microfibrillar component preferentially located in elastic matrices, J. Cell Biol. 124 (5) (1994) 855–863.

[28] E.C. Davis, Immunolocalization of microfibril and microfibril-associated proteins in the subendothelial matrix of the developing mouse aorta, J. Cell Sci. 107 (Pt 3) (1994) 727–736.

[29] N.L. Charbonneau, et al., Microfibril structure masks fibrillin-2 in postnatal tissues, J. Biol. Chem. 285 (26) (2010) 20242–20251.

[30] J. Li, et al., A novel pathogenic mutation in FBN2 associated with congenital contractural arachnodactyly for preimplantation genetic diagnosis, J. Genet. Genomics 47 (5) (2020) 281–284.

[31] J.S. Kumaratilake, et al., The tissue distribution of microfibrils reacting with a monospecific antibody to MAGP, the major glycoprotein antigen of elastin-associated microfibrils, Eur. J. Cell Biol. 50 (1) (1989) 117–127.

[32] L.Y. Sakai, D.R. Keene, E. Engvall, Fibrillin, a new 350-kD glycoprotein, is a component of extracellular microfibrils, J. Cell Biol. 103 (6 Pt 1) (1986) 2499–2509.

[33] R.B. Sterzel, et al., Elastic fiber proteins in the glomerular mesangium in vivo and in cell culture, Kidney Int. 58 (4) (2000) 1588–1602.

[34] J. Barallobre-Barreiro, et al., Extracellular Matrix in Vascular Disease, Part 2/4: JACC Focus Seminar, J. Am. Coll. Cardiol. 75 (17) (2020) 2189–2203.

[35] P.A. Gupta, et al., Ten novel FBN2 mutations in congenital contractural arachnodactyly: delineation of the molecular pathogenesis and clinical phenotype, Hum. Mutat. 19 (1) (2002) 39–48.

[36] S. Peeters, et al., The fibrillinopathies: new insights with focus on the paradigm of opposing phenotypes for both FBN1 and FBN2, Hum. Mutat. 43 (7) (2022) 815–831.

[37] J.Y. Suk, et al., Structural consequences of cysteine substitutions C1977Y and C1977R in calcium-binding epidermal growth factor-like domain 30 of human fibrillin-1, J. Biol. Chem. 279 (49) (2004) 51258–51265.

[38] D.P. Reinhardt, R.N. Ono, L.Y. Sakai, Calcium stabilizes fibrillin-1 against proteolytic degradation, J. Biol. Chem. 272 (2) (1997) 1231–1236.

[39] M.R. Davis, K.M. Summers, Structure and function of the mammalian fibrillin gene family: implications for human connective tissue diseases, Mol. Genet. Metab. 107 (4) (2012) 635–647.

[40] G. Sengle, et al., Abnormal activation of BMP signaling causes myopathy in Fbn2 null mice, PLoS Genet. 11 (6) (2015) e1005340.

[41] P. Xu, et al., A novel splicing mutation in the FBN2 gene in a family with Congenital Contractural Arachnodactyly, Front. Genet. 11 (2020) 143.

[42] X. Zhou, et al., A HAD family phosphatase CSP-6 regulates the circadian output pathway in Neurospora crassa, PLoS Genet. 14 (1) (2018) e1007192.

[43] Y. Shi, et al., Ocular phenotype of Fbn2-null mice, Invest. Ophthalmol. Vis. Sci. 54 (12) (2013) 7163–7173.

[44] S.S. Chaudhry, et al., Mutation of the gene encoding fibrillin-2 results in syndactyly in mice, Hum. Mol. Genet. 10 (8) (2001) 835–843.

[45] P.N. Robinson, M. Godfrey, The molecular genetics of Marfan syndrome and related microfibrillopathies, J. Med. Genet. 37 (1) (2000) 9–25.

[46] H.C. Dietz, et al., Four novel FBN1 mutations: significance for mutant transcript level and EGF-like domain calcium binding in the pathogenesis of Marfan syndrome, Genomics 17 (2) (1993) 468–475.

[47] I. Herskowitz, Functional inactivation of genes by dominant negative mutations, Nature 329 (6136) (1987) 219–222.

[48] E.A. Putnam, et al., Parental somatic and germ-line mosaicism for a FBN2 mutation and analysis of FBN2 transcript levels in dermal fibroblasts, Am. J. Hum. Genet. 60 (4) (1997) 818–827.

[49] P.N. Robinson, et al., The molecular genetics of Marfan syndrome and related disorders, J. Med. Genet. 43 (10) (2006) 769–787.

[50] H.C. Dietz, et al., Marfan phenotype variability in a family segregating a missense mutation in the epidermal growth factor-like motif of the fibrillin gene, J. Clin. Invest. 89 (5) (1992) 1674–1680.

[51] H.C. Dietz, et al., Clustering of fibrillin (FBN1) missense mutations in Marfan syndrome patients at cysteine residues in EGF-like domains, Hum. Mutat. 1 (5) (1992) 366–374.

[52] Q. Zhong, et al., A response prediction model for taxane, cisplatin, and 5-fluoro-uracil chemotherapy in hypopharyngeal carcinoma, Sci. Rep. 8 (1) (2018) 12675.

[53] S.Y. Kim, et al., Aberrantly hypermethylated tumor suppressor genes were identified in oral squamous cell carcinoma (OSCC), Clin. Epigenetics 11 (1) (2019) 116.